Bulletin of the Seismological Society of America, Vol. 87, No. 5, pp. 1158–1170, October 1997

The Northern San Gregorio Fault Zone: Evidence for the Timing of Late Holocene Earthquakes near Seal Cove, California

by Gary D. Simpson, Stephen C. Thompson,[1] J. Stratton Noller,[2] and William R. Lettis

Abstract The San Gregorio fault is the principal active fault west of the San Andreas fault in central coastal California, yet it remains the largest known fault in the region whose seismogenic potential is not known. In this study, we integrate traditional paleoseismic and archaeologic investigations to define the location, style, and timing of slip events on the northern San Gregorio fault at a site near Seal Cove in Moss Beach, California. The on-land portion of the San Gregorio fault at Seal Cove is a late-Holocene active dextral slip fault. Trench excavations revealed a broad zone of faulting, at least 22 m wide, consisting of five Holocene-active strands. These include a single mid-Holocene east-vergent reverse fault and four late-Holocene near-vertical strike-slip faults. The most recent event occurred after the deposition of a native Californian cooking hearth dated A.D. 1270 to A.D. 1400, but prior to the arrival of Spanish missionaries ca. 1775. The penultimate event at the site is less well constrained but appears to have occurred between A.D. 620 and A.D. 1400. The penultimate event was associated with horizontal displacement on the order of 3 m, based on reconstruction of a thrust wedge within the fault zone. The geometry of midden deposits shows a 5 $(-2, +6)$ m deflection along the projection of faults associated with the most recent event (MRE). All or part of this deflection may be associated with the MRE. These displacements are consistent with M_w 7 to 7¼ earthquakes and show that the San Gregorio fault is an active seismogenic source that should be considered in seismic hazard assessments in the San Francisco Bay area.

Introduction

The San Gregorio fault zone is the principal tectonic structure west of the San Andreas fault in the coastal region of central California between Monterey Bay and Bolinas Lagoon. The fault is located primarily offshore, with strands intersecting the coastline at only two locations: between Pt. Año Nuevo and San Gregorio, and between Pillar Point and Moss Beach (Fig. 1). The northern on-land portion of the fault zone is sometimes referred to as the Seal Cove fault, but we do not make this distinction in this article. Because of its limited onshore extent, few detailed geologic studies have been conducted to evaluate the style and rate of late Quaternary deformation along this complex fault zone. Thus, wide disparities exist in published estimates of the location, character, and paleoseismic behavior of the fault. For example, estimates on the style of deformation range from predominantly right-lateral strike slip based on offset bedrock lithologies (e.g., Hall, 1975; Graham and Dickinson, 1978; Clark *et al.*, 1984) and offset Quaternary marine terraces (e.g., Weber, 1994) to west-vergent reverse slip based on fault geometry interpreted from offshore seismic reflection data (e.g., Brocher, 1993; Lewis, 1993, 1994). Published slip-rate estimates for the San Gregorio fault range from 1 to 3 mm/yr (Sedlock and Hamilton, 1991), to 4 to 10 mm/yr (Weber, 1994), to 13 to 16 mm/yr (Clark *et al.*, 1984). There are no published estimates on the timing or number of late Holocene events. Thus, the San Gregorio fault represents the largest known active fault in the San Francisco Bay area whose seismogenic potential (i.e., slip rate, displacement per event, sense of slip, recurrence, and maximum earthquake potential) is not well known.

In this article, we provide results from a paleoseismic investigation conducted along the northern onshore reach of the San Gregorio fault near Seal Cove, in Moss Beach, California (Fig. 2). At this location, the fault trace transects a previously identified archaeological site (California registered site CA-SMA-134) and is well defined by a 1.5- to 3-m-high, east-facing fault scarp and associated sag pond. Our studies consisted of two interrelated tasks: (1) definition of the distribution and character of archaeological deposits at

[1]Present address: Department of Geological Sciences, University of Washington, Seattle, Washington 98195

[2]Present address: Department of Geological Sciences, Vanderbilt University, Nashville, Tennessee.

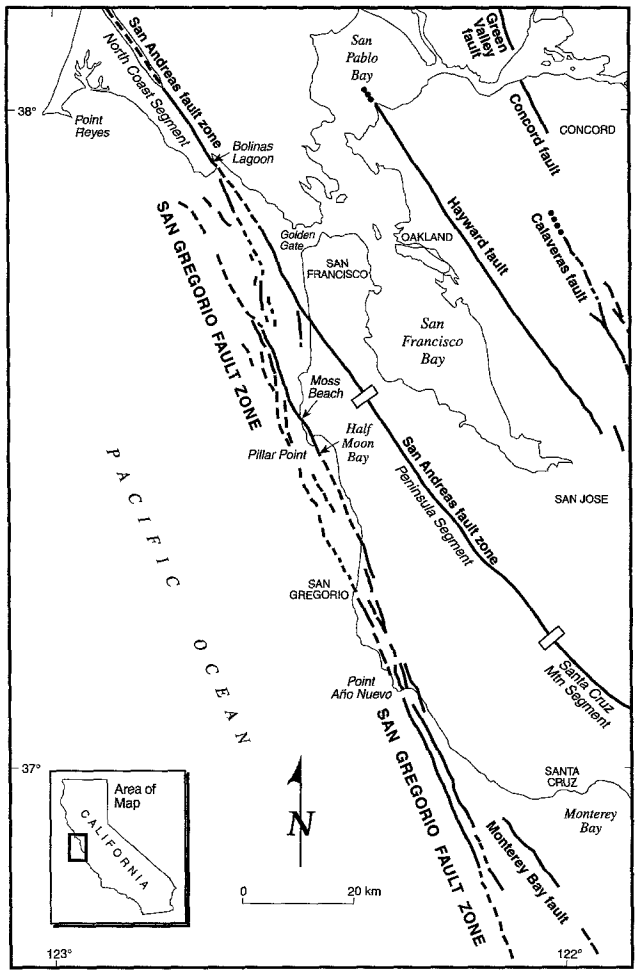

Figure 1. Map showing the San Gregorio fault zone and other major Holocene faults in the western San Francisco Bay area. Modified from Jennings (1994), segment boundaries (rectangles) along the San Andreas fault after WGCEP (1990).

the site, and (2) a paleoseismic trench investigation to document the character, number, and timing of surface-faulting events.

These investigations document primarily right-lateral strike-slip displacement along the fault with two large surface rupturing earthquakes during the past 700 to 1300 yr. Estimates on the amount of displacement during the most recent and penultimate events, combined with published estimates of slip rate, allow us to assess the amount of accrued strain on the fault since the most recent event. These data are important for estimating earthquake probabilities in the San Francisco Bay area (WGCEP, 1990), assessing regional strain-rate budgets (e.g., Kelson *et al.,* 1992), and evaluating local seismic hazards for general community planning. In addition, these data provide important constraints on the tectonic setting of the San Gregorio fault and the role of the fault in accomodating deformation along the Pacific–North American plate boundary.

Tectonic Setting

The San Gregorio fault zone is the northern part of a system of coast-parallel strike-slip faults extending from Point Conception in the south to the Marin Peninsula in the north. The southern part of the system includes the Sur, San Simeon, and Hosgri faults (Hall, 1975; Graham and Dickinson, 1978). The San Gregorio fault extends from Monterey Bay to the north, where it merges with the San Andreas fault at a complex, poorly understood intersection or right-releasing step-over between the Golden Gate and Bolinas Lagoon (Fig. 1). Because the fault zone is complex and lies primarily offshore, its rate of deformation and relative components of strike, slip, oblique slip, and/or reverse slip remains poorly understood.

The physical and behavioral connection of the San Gregorio fault with the San Andreas fault is inferred from offshore geophysical data and tectonic models based on onshore paleoseismic studies. Recent paleoseismic data from the North Coast segment (Niemi and Hall, 1992; Noller *et al.,* 1993) and Peninsula segment of the San Andreas fault (Clahan *et al.,* 1995) show an increase in slip rate of 3 to 10 mm/yr on the San Andreas fault north of the intersection with the San Gregorio fault. This increase in slip rate suggests that the San Gregorio fault is, at least in part, a strike-slip fault accomodating dextral offset at the Pacific–North American plate margin. To fully understand the partitioning of dextral slip between the Peninsula segment of the San Andreas fault and the San Gregorio fault, additional data on the Holocene slip rate of the San Gregorio fault are needed.

Available geologic, geomorphic, and geophysical data indicate that the San Gregorio fault zone is a broad, complex system of high-angle dextral strike-slip and west-vergent reverse faults. The relative distribution of strike-slip and reverse-slip displacement on the San Gregorio fault remains largely unknown however. Onshore stratigraphic and geomorphic evidence suggests the system is dominated by significant dextral slip along high-angle faults, although the rate of this movement is poorly constrained. Offset Cretaceous and Tertiary bedrock units suggest up to 115 km of dextral offset at an average late Cenozoic slip rate of 7 to 9 mm/yr (Graham and Dickinson, 1978). Clark *et al.* (1984) correlate bedrock units between Point Reyes and the Santa Cruz Mountains and estimate up to 150 km of offset, yielding an average late Cenozoic slip rate on the order of 13 to 16 mm/yr. Where the fault zone comes onshore at Point Año Nuevo, it deforms late Pleistocene marine terraces at a poorly constrained dextral slip rate of 4 to 10 mm/yr (Weber and Lajoie, 1980; Weber, 1994). In addition, there is a consistent component of west-vergent reverse faulting along the San Gregorio fault. At Point Año Nuevo, the broad fault zone is present that contains two principal dextral-slip traces and a west-vergent reverse fault. Offshore seismic reflection data suggest that the San Gregorio fault is part of a system of west-vergent thrust faults (Lewis, 1993, 1994).

The timing and recency of movement along the San

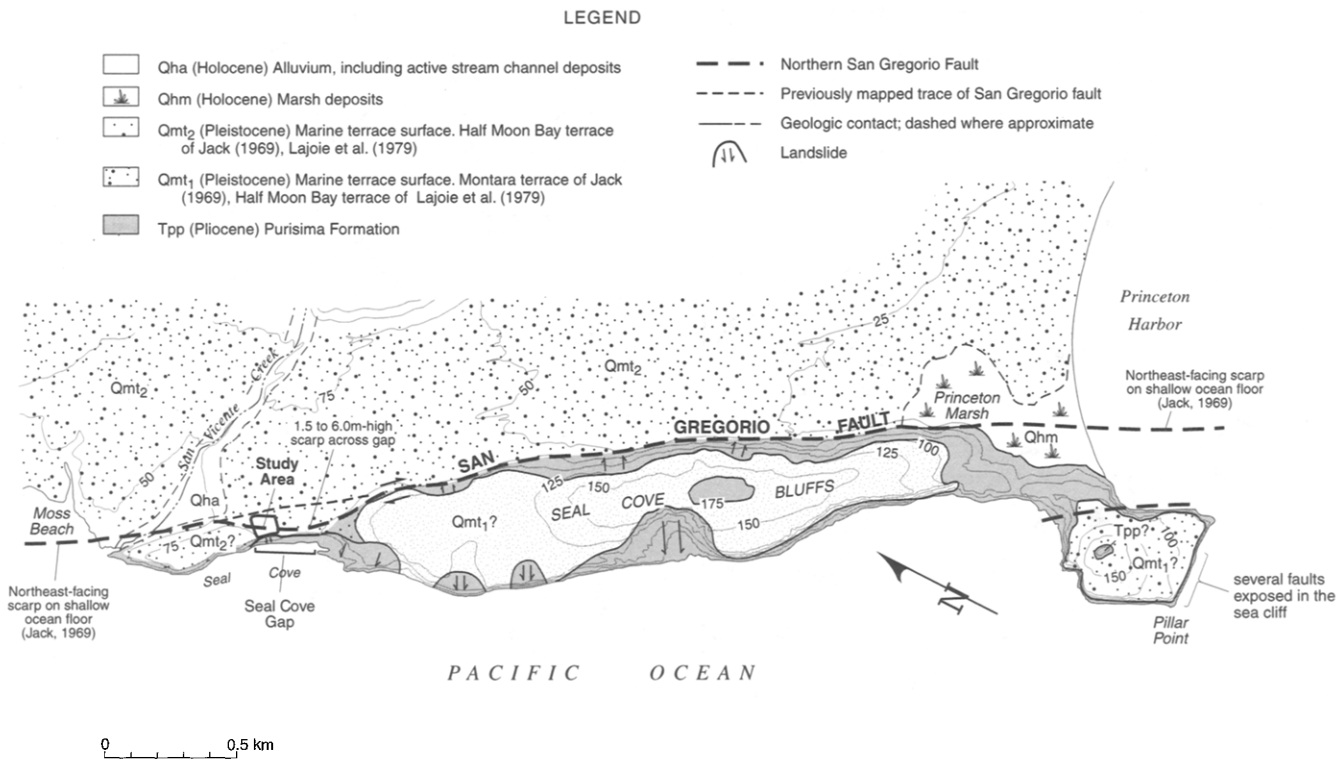

Figure 2. Generalized geologic map of the northern on-land portion of the San Gregorio fault, showing the study area and both the previously mapped and the revised fault locations.

Gregorio fault is poorly constrained. The fault trace is geomorphically well-expressed onshore by scarps, deflected drainages, offset marine terrace back-edges, and linear topographic features (this study; Weber, 1994; Weber and Lajoie, 1980; Bedrossian, 1979) and offshore by topographic and geomorphic features on the sea floor including scarps (Jack, 1969; Reed *et al.,* 1992), dewatering structures (Greene *et al.,* 1994), and aligned linear hills (Reed *et al.,* 1992). Displacement of Holocene deposits has been reported at Año Nuevo (Weber and Lajoie, 1980; Weber and Cotton, 1981; Weber, 1994), and on the alluvial fan at Denniston Creek (Weber and Lajoie, 1980). However, geodetic data do not show strain accumulating across the fault (Coppersmith and Griggs, 1978), the fault is not creeping at the surface (Galehouse, 1995), and only sparse, diffuse microseismicity is associated with the fault (Hill *et al.,* 1991). There has been no large surface faulting event on the San Gregorio fault since the arrival of Spanish missionaries ca. 1775, although Toppozada *et al.* (1981) describe two historic earthquakes that might have occurred on the San Gregorio fault, an *M* 5 to 5½ event near Pillar Point in 1856, and an *M* 5¾ to 6 event southeast of Point Año Nuevo in 1884.

Geologic and Geomorphic Setting

The northern on-land portion of the San Gregorio fault is 3 km long, extending from Pillar Point to Moss Beach (Fig. 2). The fault was exposed until recently in the sea cliff at Moss Beach (Fig. 2), where it juxtaposes sheared mudstones of the lower Pliocene Purisima Fm on the west against marine terrace sands (Half Moon Bay terrace, described below) on the east. The principal fault surface within the 30- to 40-m-wide zone at this location strikes N18-35W and dips 65 to 80E (Leighton and Associates, 1971). The steep dip and clear west-side-up vertical separation of Purisima Fm observed in the sea cliff shows that the fault is a high-angle oblique slip fault at this location.

Tectonic geomorphology of the on-land portion of the northern San Gregorio fault is consistent with west-side-up right-oblique displacement. The fault forms an east-facing escarpment up to 30 m high along the eastern margin of the Seal Cove Bluffs (Fig. 2). To the north, between Seal Cove and Moss Beach, the fault is expressed as an 18-m-high east-facing escarpment adjacent to San Vicente Creek, which appears to be deflected right laterally to the northwest. At Seal Cove, the high fault scarp is interrupted by an approximately 200-m-wide windgap, which we informally refer to as the Seal Cove gap. The fault is expressed across the gap by a small east-facing scarp 1.5 to 6 m high. Our study area is located within the Seal Cove gap.

The fault displaces and deforms the principal geomorphic surface in the area, the Half Moon Bay marine terrace (Lajoie *et al.,* 1979; Lajoie, 1986). The Half Moon Bay terrace has been correlated to the stage 5a (83 ka) sea-level

highstand (Kennedy *et al.*, 1981). East of the fault, the Half Moon Bay marine terrace surface is laterally continuous for several kilometers. The terrace is warped in a broad northeast-plunging syncline whose axis intersects the San Gregorio fault several km south of Seal Cove (Lajoie *et al.*, 1979). Remnants of a marine terrace are also preserved on the Seal Cove Bluffs west of the San Gregorio fault. The age of this terrace has not been documented, and correlation of the terrace to the Half Moon Bay terrace east of the fault is uncertain. Jack (1969) interprets the terrace on Seal Cove Bluffs (which he calls the Montara terrace) to be older than the Half Moon Bay terrace. This interpretation requires that Seal Cove Bluff was an island during development of the Half Moon Bay terrace. Lajoie *et al.* (1979) correlate the Seal Cove Bluff terrace west of the fault with the Half Moon Bay terrace to the east and suggest that the Seal Cove Bluff has been uplifted via tectonic deformation. They use an analysis of boreholes and bathymetry to conclude that the abrasion platform west of the fault has been warped and uplifted into a relatively steep-sided structural dome, which is truncated on its eastern side by the San Gregorio fault, forming the high escarpment along the Seal Cove Bluffs. If the uplifted abrasion platform west of the fault is the Half Moon Bay terrace, the platform has been displaced vertically some 50 m in the past 83,000 years based on the depth of the Half Moon Bay terrace abrasion platform east of the fault (Weber and Lajoie, 1980). This scenario suggests a vertical separation rate of up to 0.6 mm/yr. Uplift or shortening along the fault indicates a localized restraining bend or step-over along the San Gregorio fault.

Across the Seal Cove gap, the abrasion platform west of the fault (e.g., Seal Cove Bluff terrace) may extend or be eroded beneath sea level, based on observation of seacliff exposures (Jack, 1969) that are presently obscured by landslides. The gap therefore appears to represent either an infilled paleochannel or, alternatively, represents a sharp structural down-warping of the Seal Cove Bluff terrace surface. The alluvial character of the sediments west of the fault exposed in our trench and in limited exposures in the sea cliff at Seal Cove support the interpretation that the Seal Cove gap is a paleochannel. These alluvial deposits are distinct from marine/littoral sediments exposed in the sea cliff just northwest of the gap.

Prior to this study, the precise location of the San Gregorio fault within the Seal Cove gap was poorly constrained because of the lack of a large, distinct scarp or other well-defined geomorphic features. In this study, we refine the location of the fault across the gap based on the results of our trenching study, a compilation of previous trenching studies, and detailed assessment of subtle geomorphic features. Previous mapping of the San Gregorio fault (Glen, 1959; Jack, 1969; Weber and Lajoie, 1980; Brabb and Pampeyan, 1972; Pampeyan, 1994) shows the fault as a straight projection across the Seal Cove gap between the large east-facing scarps to the north and south (Fig. 2). This inferred projection was adopted as the active fault trace for the State of California's Alquist-Priolo Earthquake Fault Zone map. Our review of consultant reports (e.g., Wood, 1983; JCP Associates, 1987; Cleary Consultants, 1990), however, suggests that the main trace of the fault arcs westward across the topographic gap at Seal Cove (Fig. 2). This alignment is coincident with a 1.5- to 6-m-high east-facing scarp that can be traced across the entire gap. Our trench, as well as previous consultant trenches across this scarp, shows a distinct lithologic break across the fault indicative of significant cumulative displacement. Conversely, consultant trenches across the previously mapped straight-line projection of the fault revealed only fractures and secondary faults with minor displacements that do not juxtapose dissimilar strata. Based on the results of our study, we conclude that the main San Gregorio fault follows an arcuate path across the Seal Cove gap marked by a distinct, yet relatively low, east-facing scarp.

Additional strands of the northern San Gregorio fault may cross Pillar Point and extend just offshore of Seal Cove (Fig. 2). This interpretation would be consistent with the character of the fault at Point Año Nuevo and offshore, where it is a broad zone consisting of multiple active traces. If the on-land fault trace described herein is part of a broader fault zone at Seal Cove, it would represent the eastern limit of the zone, and other faults would lie offshore to the west. With the possible exception of a small west-facing scarp across the Holocene alluvial fan of Denniston Creek 1 km to the east (Weber and Lajoie, 1980), there are no significant traces within the fault zone east of the main on-land trace of the northern San Gregorio fault shown in Figure 2. The distribution, level of activity, and sense of displacement of offshore faults are not known.

Site Description

Our study area is located on the bluff-top directly east of Seal Cove, at the southern edge of the Fitzgerald Marine Reserve within the community of Moss Beach (Figs. 2 and 3). At this site, the fault trace is marked by a low, 1.5- to 3.0-m-high east-facing scarp across a previously identified archaeological site (CA-SMA-134). The eastern, downthrown side of the fault at this site is bordered by a broad depression, probably a tectonic sag, that contains hydrophytic vegetation. The 2500-m^2 archaeological site is a midden containing shell, bone, cooking stones, tools, and other debris from prehistoric human occupation (Hylkema, 1996). The archaeological site extends from the sea cliff eastward across the fault scarp and into the depression.

The study area is within the Seal Cove gap described above, at an elevation of 18 to 21 m (60 to 65 ft) above mean sea level. Seacliffs 20 m northwest of the gap expose approximately 10 m of marine terrace deposits consisting of bedded, well-sorted sand, clayey sand, and gravel overlying an abrasion platform eroded into sheared Purisima mudstone. Within Seal Cove itself, however, active landsliding and slumping of the cliff face have obscured exposures of

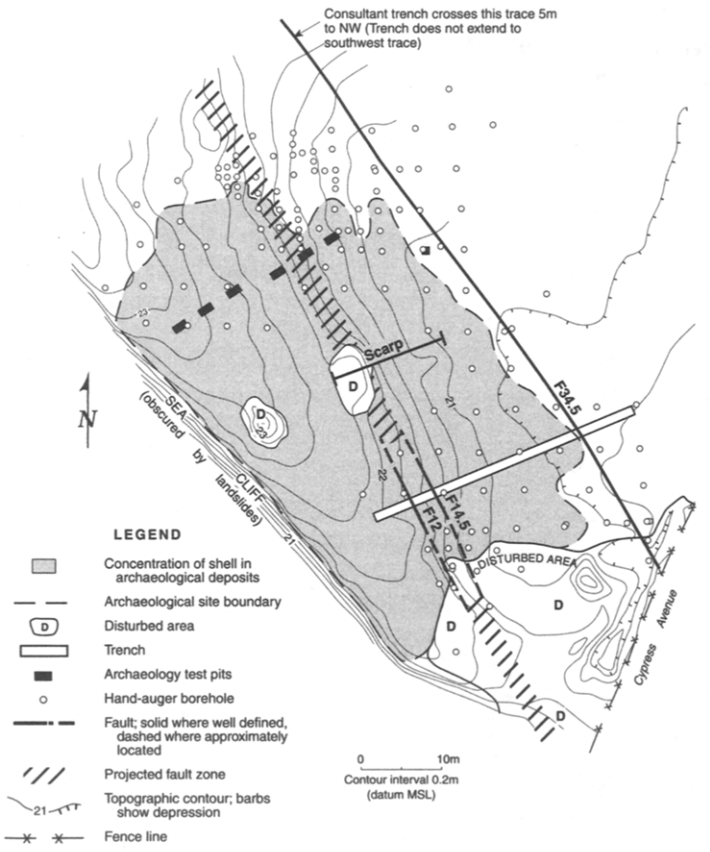

Figure 3. Site map showing the Seal Cove archaeological site (CA-SMA-143) transected by the northern San Gregorio fault. Archaeological test pits were excavated along the entire length of the trench prior to the trench excavation.

the platform and/or paleochannel and most of the overlying sediments.

Methods

Our approach in this study was to integrate the results of archaeological and paleoseismological investigations to provide a record of past earthquakes at the Seal Cove site. The use of archaeology augments the more traditional geology-based techniques (i.e., mapping and trenching) typically used in paleoseismological studies. The midden at the Seal Cove site is a spatially definable, layered, datable deposit, and we utilized both the outer margin of the midden and strata within the midden to provide additional data on the timing and character of past surface-rupturing earthquakes.

The distribution of cultural artifacts at the site was defined by shovel-probe surveys and the analysis of 145 hand-auger borings. In addition, two archaeological test pit transects were excavated across the scarp, one along the alignment of the paleoseismic trench, to characterize the midden (e.g., define artifact, floral, and faunal assemblages, determine the age of the site, and define ethnostratigraphic features) (Fig. 3).

Following the archaeological studies, we excavated a single 36-m-long, 3- to 3.5-m-deep trench to determine the location, nature, and timing of surface-rupturing earthquakes on the San Gregorio fault. The trench was excavated across the fault scarp and into the tectonic sag. It extended through the archaeological midden. The trench location was selected based on the distribution of archaeological material, location of the scarp, and potential presence of fine-grained layered deposits within the sag.

Samples of charcoal, humus-rich units (buried soil A horizons), and marine bivalves were submitted for radiocarbon analysis (Table 1). Following material-specific corrections, the radiocarbon analyses were dendrochronologically corrected to calibrated years according to the procedure of Stuiver and Reimer (1993). We recognize the suspect nature of radiocarbon analysis of buried soil A horizons and shell. Soils can include unknown amounts of older, miniscule detrital charcoal, as well as younger roots and organic acids. Young carbon can disproportionately influence a sample's age; therefore, we treat the age estimates on organic-rich soils and sediments as minimum ages. Radiometric dating of *Mytilus Californianus* (mussel) shells at the site gave internally consistent ages. Radiocarbon ages of stratigraphically equivalent samples of charcoal (RC201) and *Mytilus Californianus* (RC124, RC122, RC13) varied by about 680 ^{14}C years and is within the range of reservoir ages (ΔR = 75 to 275 ^{14}C yr, where ΔR is an additive correction to a global average 400 ^{14}C yr ocean reservoir age) for marine

Table 1
Radiocarbon Analytical Data for the Seal Cove Site

Sample*	Unit**	Geologic Material	Radiocarbon age ± 1σ (^{14}C yr B.P.)†	δ^{13}C (‰)‡	ΔR (^{14}C ± 1σ)§	Calibrated Age (cal yr)¶
B-74109	Ap	*Mytilus californianus*				A.D. 1070–1330
RC12	[D]	shell	1410 ± 60	0.0	225 ± 35	(880–620 B.P.)
B-74112	Ap	*Mytilus californianus*				A.D. 1180–1420
RC123	[D]	shell	1330 ± 60	0.0	225 ± 35	(770–530 B.P.)
B-74113	Ap	*Mytilus californianus*				A.D. 1070–1330
RC124	[C]	shell	1410 ± 60	0.0	225 ± 35	(880–620 B.P.)
B-74111	Ap	*Mytilus californianus*				A.D. 1220–1420
RC122	[C]	shell	1310 ± 50	0.0	225 ± 35	(730–530 B.P.)
B-74110	Ap	*Mytilus californianus*				A.D. 1170–1430
RC13	[C]	shell	1320 ± 70	0.0	225 ± 35	(780–520 B.P.)
B-85776	Ap					A.D. 1270–1400
RC201	[C]	Charcoal‖	680 ± 50	−22.5	—	(680–550 B.P.)
B-72614		Surface soil				A.D. 1160–1290
RC106	Acum	A horizon	810 ± 50	−25.0	—	(790–660 B.P.)
B-72613		Buried soil A				A.D. 620–830
RC104	IIAb	horizon	1330 ± 60	−25.0	—	(1330–1120 B.P.)
B-72617		Organic bond				4850–4540 B.C.
RC116	Qp	clay	5850 ± 70	−25.0	—	(6800–6490 B.P.)

*Laboratory number (B = Beta Analytic, Inc.) and field sample number (RC).

**Acum, Ap, IIAb = pedostratigraphic units; [C], [D] = ethnostratigraphic units; Qp = Quaternary pond deposit.

†All analyses performed by the conventional radiometric technique using a half-life of 5568 yr. Reported ages are corrected for δ^{13}C and include a laboratory error multiplier of 1.0 in reported laboratory uncertainty.

‡Estimated value used, ‰ is parts per mil (thousand).

§We used a ΔR that is representative of Holocene marine shells taken from the central California coast (Stuiver *et al.*, 1986). ΔR value is in addition to a global average 400-yr oceanic reservoir correction.

¶Calibrated using the program CALIB 3.0.3c, probability distribution Method B (2σ area), from Stuiver and Reimer (1993). B.P. is years before present referenced to 1950.

‖Recovered from core of hearth during archaeological investigation.

mussel shell along this coast (Stuiver *et al.*, 1986, from Berger *et al.*, 1966; Robinson and Thompson, 1981). Because the uncertainty in reservoir age is large, however, we defer to the charcoal age for temporal control of midden-bearing deposits.

Trenching Investigations

Overview of Trench Results

The trench exposes two major Holocene-active faults of the northern San Gregorio fault zone (Fig. 4). These faults juxtapose distinctly dissimilar sections of marine terrace and alluvial deposits, demonstrating that the trench crossed the primary on-land fault zone (Fig. 2). The terrace deposits consist of near-shore marine deposits that, as described above, probably are associated with the 83 ka Half Moon Bay terrace. Alluvial deposits are present west of the fault zone, within the paleochannel associated with the Seal Cove gap. The age of these deposits is not known. These marine and alluvial deposits were extensively deformed by faulting, locally eroded, and subsequently buried by Holocene colluvium, pond sediments, and organic-rich soils that locally contain midden debris.

A hiatus of unknown length is recorded in the trench stratigraphy by an unconformity separating the older marine and alluvial deposits from the overlying sequence of Holocene sediments. The unconformity atop the terrace deposits at either end of our trench is marked by a buried A/E/Bs soil profile developed in the basal Holocene and upper late Pleistocene terrace sediments. This soil profile represents leaching of perhaps generations of overlying soils and formation of a clay hardpan on the top of the terrace sediments. The A/E/Bs soil profile is not developed in the central part of the trench where soil formation appears to have been impeded by continued tectonic subsidence and pond sedimentation. Holocene deformation is represented by four near-vertical strike-slip fault strands that deform the unconformity and extend into the overlying mid to late Holocene sediments (faults at meter 11.9, 12.1, 14.5, and 34.5; Figs. 4, 5, and 6) and an east-vergent reverse fault that deforms the unconformity and overlying pond deposits (meter 18; Fig. 4).

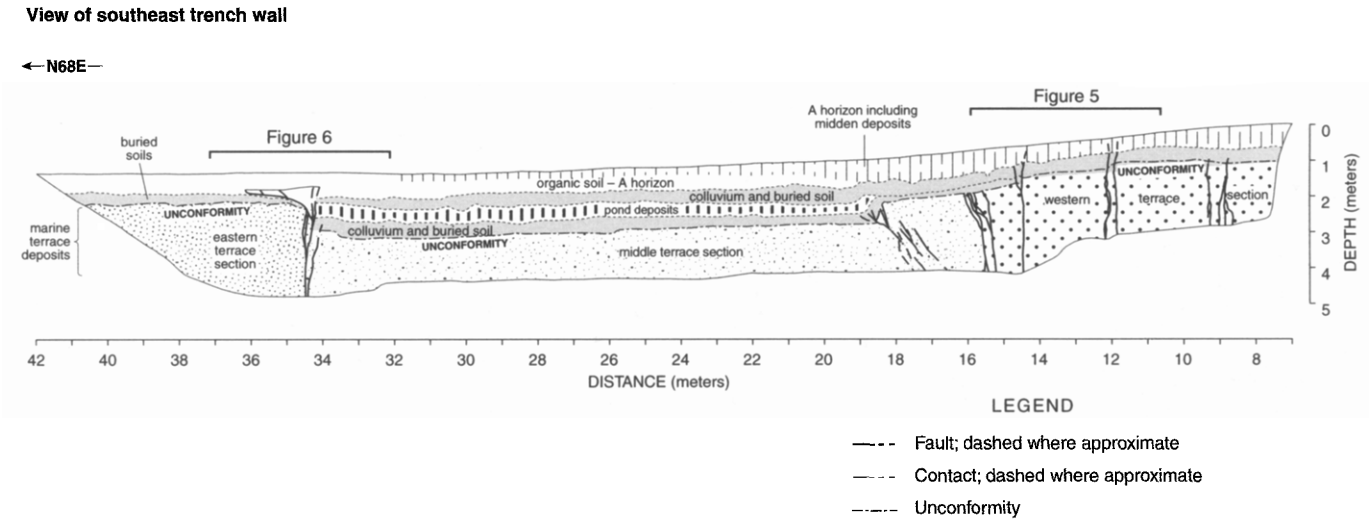

Figure 4. Schematic log of the Seal Cove trench, view to the southeast, showing principal stratigraphic groups and faults. Horizontal scale is tied to an arbitrary survey station 7 m southwest of the end of the trench.

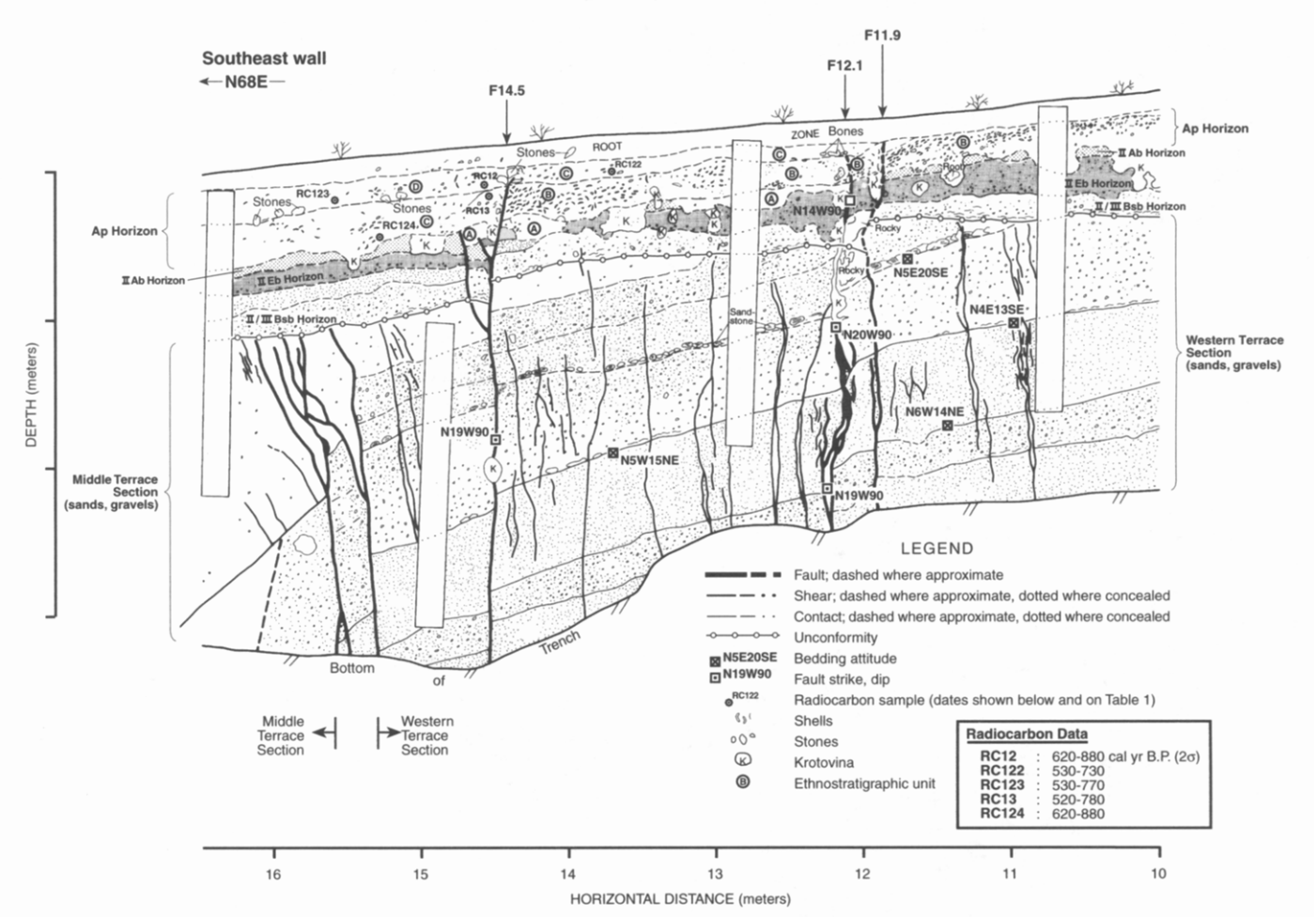

Figure 5. Detail log of the western part of the Seal Cove trench.

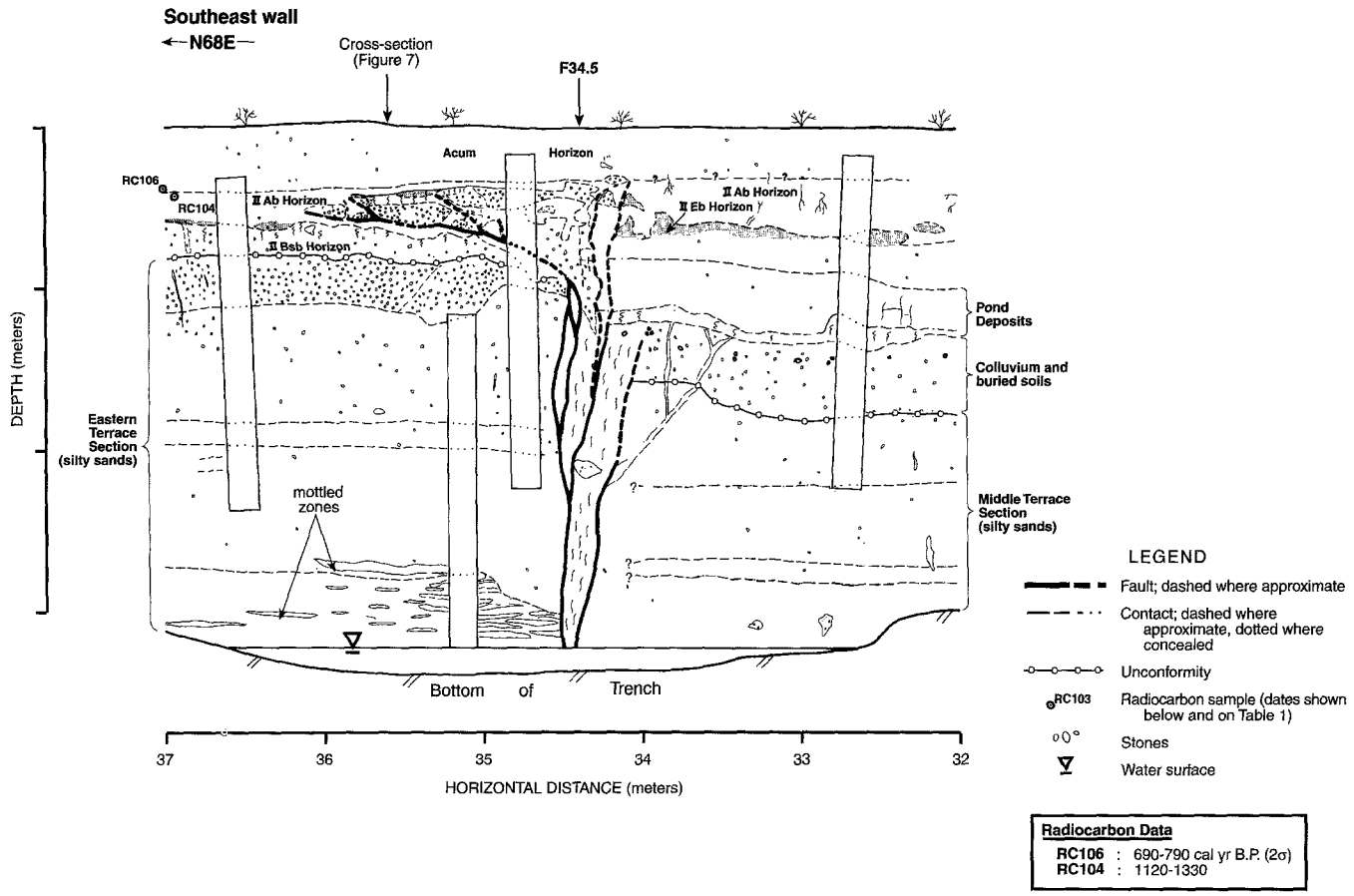

Figure 6. Detail log of the eastern part of the Seal Cove trench.

Within the trench, we define three types of units: lithostratigraphic, pedostratigraphic, and ethnostratigraphic units. The most fundamental of these are the lithostratigraphic units, upon which soils have formed (pedostratigraphic units) and midden debris incorporated (ethnostratigraphic units). These unit designations are not distinct, in that pedostratigraphic units are superimposed onto the uppermost lithostratigraphic units, and all of the ethnostratigraphic units are contained within the youngest lithostratigraphic and pedostratigraphic units. Definition of these three distinct stratigraphic unit types is necessary in this study because each represents a unique time period from the late Pleistocene through the late Holocene and allows us to assess distinct periods of deformation within the trench. A description of the unconformity that separates the late Pleistocene and Holocene sediments is included within the discussion of lithostratigraphic units.

Lithostratigraphic Units

Older marine and alluvial deposits in the trench, below the prominent unconformity, are present in three distinct, tectonically juxtaposed stratigraphic sections (Fig. 4). In this discussion, we informally refer to these as the western, middle, and eastern terrace sections. The western section, southwest of meter 15.5, consists of 25- to 60-cm-thick interbeds of moderately to well-sorted sand and poorly sorted gravel. The gravel beds are composed of subrounded feldspar and quartz pebbles locally derived from the Cretaceous Montara Granodiorite. A single clayey sand bed is present at the top of the western section. We interpret the deposits of the western terrace section to be interbedded littoral sand and alluvial gravels associated with the infilling of the paleochannel within the Seal Cove gap. Since the age of the Seal Cove Bluff terrace, into which the paleochannel is apparently eroded, is not known, the age of the alluvial deposits in the western terrace section is also uncertain. The western and middle terrace sections are juxtaposed by a complex zone of near-vertical faults at meter 15.5.

Deposits associated with the infilled Seal Cove paleochannel are not present east of the western zone of faults in the trench. The paleochannel has presumably been faulted laterally away from Seal Cove. As such, the deposits of the middle and eastern terrace sections are distinct from the western section. The middle and eastern terrace sections (Fig. 4) consist of deposits that are distinctly finer-grained than those in the western section. The deposits are faintly bedded to massive sandy and clayey silts with sparse randomly distributed feldspar and quartz pebbles. These sediments are olive to blue-gray, with diffuse mottling. We interpret the middle and eastern terrace sections to be marine

littoral deposits of the 83 ka Half Moon Bay terrace. The middle and eastern sections are juxtaposed by a vertical fault at meter 34.5.

The distinct unconformity occurs at the top of the older marine and alluvial deposits and represents a significant hiatus in the depositional record (Fig. 4). Broad constraints on the age of the unconformity can be derived from the nature of the overlying and underlying strata, the degree of deformation prior to and subsequent to the unconformity, and the degree of soil–profile development on the unconformity. A maximum age for the unconformity is constrained by the age of the underlying deposits, which, as described above, probably are Half Moon Bay terrace deposits in the middle and eastern terrace sections and, therefore, were deposited about 83 ka. The deposits of all three terrace sections were faulted extensively prior to erosion and formation of the unconformity, however, which should further constrain the maximum age. The western terrace section, for example, was tilted significantly prior to formation of the unconformity. Furthermore, the western and middle terrace sections consist of distinctly dissimilar stratigraphic sections representing different sedimentary environments. These sections are juxtaposed by faults at meter 15.5 that predate the unconformity. We interpret that this preunconformity deformation occurred over a period of a few tens of thousands of years after deposition of the terrace deposits about 83 ka. An estimate of the minimum age for the unconformity is provided by the deposits and soils that overlie it. The unconformity is overlain in the central part of the trench by 0.25 to 0.5 m of gravelly colluvium, which in turn are overlain by pond deposits that are dated at 6490 to 6800 years (see below). Soil development above the unconformity (also described below) probably represents several thousands to a few tens of thousands of years. Therefore, the unconformity is likely a pre-Holocene feature.

The unconformity is tectonically down-dropped in the central part of the trench (Fig. 4). Sedimentary fill within the depression includes gravelly sandy silt colluvium that grades upward into a 25- to 40-cm-thick section of pond deposits. These pond sediments consist of two distinct clay layers: (1) a lower clay that is olive-colored and poorly bedded and (2) an upper clay that is organic rich, massive, and very dark brown to black. These two layers are separated by an abrupt, irregular contact marked by "tongues" of black clay that penetrate downward into the underlying olive clay. These clay tongues may be tectonic fissure-fill deposits or dessication crack infillings. Radiometric dating of a bulk sample of the upper organic clay (RC 116) yielded a minimum age estimate of 6490 to 6800 cal yr B.P. (ca. 4850 to 4540 B.C.; Table 1). The clayey pond sediments, in turn, grade upward into a 30- to 40-cm-thick, slightly consolidated, very dark reddish brown silt representing the gradual infilling of the pond and transition to a seasonal marsh.

The entire trench exposure is capped by up to 75 cm of loose, black sandy silt (Fig. 4). Midden debris is concentrated in this surficial deposit at the western end of the trench but grades out east of meter 23. The silt probably is deposited at the site as loess.

Pedostratigraphic Units

We recognize three pedostratigraphic units in our trench: the surficial cumulic soil and two distinct buried soils. The oldest buried soil exposed in the trench is a IIIBsb2 horizon that formed on the unconformity eroded across the marine terrace sediments. The soil is stripped of its overlying solum on the scarp face in the western part of the trench and is buried by colluvium and mid-Holocene or older pond deposits (ca. 4850 to 4540 B.C., or older) east of the scarp in the sag pond.

The IIIBsb2 horizon is overprinted by a second buried soil, a II(A/E/Bs)b profile. The lower part of the profile, the IIBsb horizon, overlaps the IIIBsb2 at the western end of the trench. Where superimposed, these two horizons form a dark reddish brown to orange clay- and sesquioxide-rich hardpan. The complex morphology of the hardpan in the western part of the trench is interpreted to be polygenetic and could not have been developed in sole association with the overlying II(A/E)b horizons.

The IIEb horizon grades from a well-developed 20- to 25-cm-thick clay-, sesquioxide-, and organic-poor horizon on and west of the fault scarp to a thin ($\leqq$10 cm), weak juvenile elluvial E horizon within the sag pond. The top of the IIEb horizon in the pond area is irregular and suggests that it and its associated A horizon have been mixed by rodent activity into the superjacent deposits and soil. We interpret this E horizon to be buried because it is present significantly deeper than E horizons in similar settings along this coast (R. Arkley, personal comm., 1994).

The third and youngest pedostratigraphic unit is the surficial A horizon. This A horizon grades from cumulic (Acum) east of the fault scarp to anthropic (Ap) at, and west of, the fault scarp. The Acum horizon is a thick, dark brown, organic sandy silt that developed within the sag pond. The Ap horizon is a thin, black, root-bound shell- and stone-rich sandy silt developed on the archaeological midden deposit. Both horizons are highly bioturbated.

Ethnostratigraphic Units

The western 23 m of our trench exposed midden deposits within the uppermost soil (Ap unit). The deposits consisted of concentrated zones of shell, bone, and stone artifacts within loose, organic surficial soils (Hylkema, 1996). We defined four ethnostratigraphic units within the trench based on the distribution of shell, bone, and lithic artifacts (Fig. 5). The oldest ethnostratigraphic unit, unit A, contains very limited midden debris. It is present directly above, and locally penetrates into, the IIEb pedostratigraphic horizon described above. The age of this unit is not known.

Unit B is a distinct shell-rich horizon that progressively increases in shell content eastward where it becomes virtually shell supported. Unit B is truncated by a vertical fault at meter 14.5 and is not present farther east. The age of this

unit is not known, although based on its archaeological context and similarity in color and texture, it is likely associated with and very close in age to the overlying unit, unit C.

Unit C is defined based on the abundance of lithic artifacts (e.g., fire-cracked rocks and pitted stones) and an obvious decrease in the concentration of shell debris relative to unit B. The abundance of cooking stones and bone in this unit indicates that it is a large-scale hearth feature (Hylkema, 1996). Unit C is offset laterally and down to the east by the fault at meter 14.5. A charcoal sample (RC 201) from the hearth submitted for radiocarbon analysis yields an age estimate of 550 to 680 cal yr B.P. (A.D. 1270 to 1400; Table 1), which is consistent with three dates from samples of *Mytilus Californianus* shell (RC 122, 124, 13) from within the hearth.

Unit D is similar to unit C in artifact assemblage and shell age; however, we differentiate it based on a lower abundance of artifacts and the presence of a distinct stone and bone line at the base of the unit. The stones and bones appear to represent a basal lag deposit. Unit D extends eastward from a poorly defined zone that abuts the fault, or a degraded scarp associated with the fault, at meter 14.5. We interpret that unit D is reworked colluvial material derived from unit C.

Paleoseismic Investigation

The trench excavation exposed a series of vertical strike-slip faults and a single west-dipping reverse fault (Figs. 4, 5, and 6). Fault strikes range from N19°W to N35°W. The two principal fault zones (at meters 15.5 and 34.5) juxtapose dissimilar sections of older marine (83 ka) and alluvial deposits, reflecting large amounts of cumulative lateral offset. Most of the deformation that we observe in the trench predates the unconformity developed on the older deposits. We are unable to differentiate distinct events within this record of older deformation, although the complexity and amount of deformation requires multiple events. Four near-vertical fault strands offset the unconformity and can be traced into the overlying late Holocene soils (at meters 11.9, 12.1, 14.5, and 34.5), representing the most recent and penultimate events. In addition, the west-dipping reverse fault at meter 18 clearly deforms the unconformity and the margin of the overlying mid-Holocene pond deposits. We use the lithostratigraphic and ethnostratigraphic relations described above to interpret the timing of late Holocene events on the San Gregorio fault.

Most Recent Event

The most recent surface rupturing earthquake (MRE) on the San Gregorio fault at Seal Cove occurred sometime after the formation of the native Californian cooking hearth (ethnostratigraphic unit C) between A.D. 1270 and 1400 (RC 201; Table 1) and prior to the arrival of Spanish missionaries ca. A.D. 1775. The MRE occurred on the fault at meter 14.5 (Fig. 5), a vertical N20°W-striking strike-slip fault with an apparent east-side-down component of separation (7 to 20 cm). We interpret strike-slip displacement on the fault because of its vertical dip and the truncation of a distinct shell-rich bed (unit B) within the midden that suggests lateral offset. No striations were observed along the fault plane. The fault at meter 14.5 is probably a single-event trace because of the simple nature of the shear plane (e.g., a single plane) and because the amount of apparent vertical separation is similar in units of different age (e.g., units above and below the unconformity). The fault can be clearly traced upward into the midden-bearing soil layers, where it truncates ethnostratigraphic unit B and displaces unit C down to the east by up to 20 cm (Fig. 5). Given that no historic surface-rupturing earthquake is known to have occurred on the San Gregorio fault since the arrival of Spanish missionaries ca. A.D. 1775, the MRE on the fault occurred sometime between A.D. 1270 and 1775.

A pair of vertical faults similar to the fault at meter 14.5 is present near meter 12 (11.9, 12.1; Fig. 5). These faults also offset the unconformity and can be traced upward into midden deposits. They displace ethnostratigraphic unit B based on distinct differences in shell concentrations across the faults. It is not known whether one or both of these faults ruptured concurrently with the fault at meter 14.5. The timing of the formation of the faults at meter 12 is constrained by the same factors as the fault at meter 14.5; they formed after the deposition of the hearth feature (A.D. 1270 to 1400), but before A.D. 1775. Although we cannot rule out multiple events, due to the proximity and similarity of the faults, we conclude that the faults at meter 12 probably ruptured during the MRE contemporaneously with the offset at meter 14.5. Alternatively, the faults at meter 12 may represent a second post-A.D. 1270 to 1400 event.

Penultimate Event

The penultimate event is expressed on the easternmost fault at meter 34.5 (Figs. 4 and 6). This fault strikes N34°W, displays a distinct flower structure, and juxtaposes dissimilar marine terrace strata in the lower part of the trench exposure. Striations on polished shear planes on this fault indicate pure strike-slip to right-oblique slip (rake of 0° to 20° N). The fault truncates the eastern margin of the mid Holocene pond deposits.

On the south wall of the trench, west-dipping splays of the fault at meter 34.5 flatten upward in the upper 1 m of the trench. Blocks of the upper part of the Pleistocene marine terrace section have been thrust over the basal part of the late Holocene IIAb soil horizon along the east-vergent splay (Fig. 6). The thrust wedge is overlain by the youngest pedostratigraphic unit, the cumulic A horizon, which is undeformed. The cumulic A horizon must postdate the penultimate event because its basal contact does not reflect the large

amount of apparent vertical displacement that would accompany the emplacement of the underlying thrust wedge. The penultimate event is therefore stratigraphically distinct from the most recent event, because the undeformed A horizon at meter 34.5 is laterally continuous with the midden-bearing soil (Ap horizon) that is faulted at the west end of the trench.

The timing of the penultimate event is constrained by the ages of the overlying cumulic A horizon and the underlying IIAB horizon. A radiocarbon date on a bulk soil sample from the surficial cumulic A horizon at meter 37 (RC 106; Fig. 6) yields a minimum age estimate of 660 to 790 cal yr B.P. (A.D. 1160 to 1290; Table 1). This age is consistent with radiocarbon ages from charcoal (RC 201; 550 to 680 cal yr B.P.) and shell within the midden deposit (Fig. 5), which supports the interpretation that the soil is laterally continuous across the site (Fig. 4). To avoid the inherent uncertainties of the bulk soil date on the cumulic A horizon at meter 37, we defer to the charcoal date (RC 201) to provide an accurate minimum constraining age for the penultimate event. The penultimate event, therefore, occurred prior to 550 cal yr B.P. (A.D. 1400). Our ability to constrain the maximum age of the penultimate event is based solely on radiocarbon analysis of a bulk soil sample from the organic-rich IIAB horizon. This analysis of RC 104 (Fig. 6) yields an age estimate of 1120 to 1330 cal yr B.P. (A.D. 620 to 830; Table 1). As discussed above, the true sample age could be much older. However, because of the relatively close correlation between the charcoal (RC 201) and bulk soil dates (RC 106) from the overlying cumulic A horizon (the bulk soil date is actually slightly older than the charcoal date), we conclude that the bulk soil date for the IIAB horizon provides a reasonable estimate of the unit age. With consideration of the appropriate uncertainties, we conclude that the penultimate event probably occurred after A.D. 620. The penultimate event, therefore, probably occurred between A.D. 620 and A.D. 1400.

Other Postunconformity Events

Additional Holocene deformation occurred along the east-vergent reverse fault at meter 18, where a diffuse 30-cm-wide shear zone deforms the unconformity and the western margin of the 6490- to 6800-yr-old (or older) pond deposits (Fig. 4). The fault does not visibly extend into deposits overlying the pond sediments. Reverse movement on the fault has deformed the unconformity into a distinct square-hinge fold.

Other Holocene slip events also have occurred on the fault at meter 34.5, but evidence for distinct events was not preserved in our trench. Evidence for repeated Holocene movement and significant cumulative offset at meter 34.5 includes the complex nature of the fault, the presence of highly sheared gouge, and truncation of the mid Holocene pond sediments.

Preunconformity Deformation

The most apparent evidence of preunconformity deformation is the substantial eastward tilting of late Pleistocene alluvial sediments that comprise the western terrace section (Fig. 5). Significant faulting occurred between meters 15 and 16, across which the western and middle terrace sections are juxtaposed. Displacement across the near-vertical faults in this area resulted in significant apparent down-to-the-east displacement (Figs. 4 and 5). Secondary faults and fractures are present throughout the western terrace section that terminate at the unconformity. In addition, the juxtaposition of dissimilar terrace sections (the middle and eastern sections) across the fault at meter 34.5 implies substantial cumulative lateral offset. All of this deformation occurred following deposition of the older marine terrace and alluvial deposits about 83 ka and prior to development of the unconformity.

Displacement per Event

The displaced wedge of terrace sand within the flower structure at meter 34.5 provides an ideal stratigraphic piercing point to measure the amount of coseismic surface displacement during the penultimate event at the site (Figs. 6 and 7). Because the wedge is exposed on both walls, we can geometrically reconstruct the shape of the wedge and the amount of slip required to restore the offset wedge to its original position. The leading-edge (northern) tip of the overthrust wedge at meter 34.5 is present on the north wall of our trench. By projecting across the trench from the wedge tip to the base of the wedge exposed on the south trench wall, and then to the inferred point of detachment south of the southern trench wall, we estimate the amount

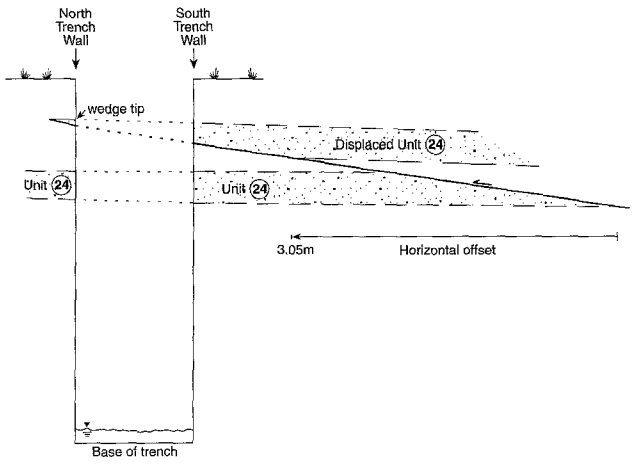

Figure 7. Cross-sectional view of trench showing location of displaced wedge within flower structure at meter 34.5 (see Fig. 6), the inferred wedge tip on the north trench wall, and the bed (unit 24) from which it was detached. The thrust fault shown is secondary to the main strike-slip fault, which is in the plane of the article.

of displacement associated with the penultimate event (Fig. 7). Based on this projection, we calculate a *horizontal* displacement of 3 ($\pm$0.2) m. This estimate assumes that (1) the exposure on the north trench wall is, indeed, the wedge tip; (2) the bed from which the wedge is removed is horizontal and tabular (the bed is very nearly horizontal across the trench); and (3) the displacement occurred in a single event. Our error encompasses the geometric uncertainties of the projection. Based on published regressions correlating displacement with earthquake magnitude, this estimate of the amount of displacement during the penultimate event is consistent with an earthquake on the order of *M*7 (Fig. 11 in Wells and Coppersmith, 1994).

Because the most recent event offsets midden deposits in the trench, the areal distribution of midden materials across the site should reflect the lateral displacement associated with the event. We estimate the map-view geometry of the midden at the site based on the results of 145 shallow hand-auger borings (Fig. 3). Based on the presence/absence and concentration of midden materials in the boreholes, the northern margin of the midden deposit appears to be deflected in a right lateral sense about 5 (-2, $+6$) m. The southern margin of the site has been disturbed by man. Deflection of the northern site margin is coincident with the fault scarp and lies along the projection of faults exposed in the trench that displaced midden-bearing strata during the most recent event (i.e., faults at meter 12 and 14.5 in the trench). All of this displacement apparently occurred in the most recent event 220 to 730 years ago and suggests an event in excess of *M*7 (Wells and Coppersmith, 1994).

Accumulation of Strain

Strain has been accumulating on the fault since the time of the most recent earthquake about 220 to 730 years ago. Although the rate of accumulation is not well constrained, published estimates from offset marine terraces range from 4 to 10 mm/yr (e.g., Weber, 1994). Below, we show the amounts of accrued strain on the fault for a range of slip rates:

Slip Rate	Accrued Strain (220 to 730 years)
4 mm/yr	0.9–2.9 m
6 mm/yr	1.3–4.4 m
8 mm/yr	1.8–5.8 m
10 mm/yr	2.2–7.3 m

These estimates of accrued strain suggest that the San Gregorio fault may have accumulated sufficient strain to produce a surface-faulting earthquake similar in size to the most recent events on the fault. We note that presumed traces offshore to the west are accomodating an unknown proportion of the overall strain.

Conclusions

Our integrated paleoseismologic and archaeologic investigations at Seal Cove demonstrate that the on-land portion of the San Gregorio fault is a late Holocene-active strike-slip fault. The most recent event on the fault occurred sometime after a native American cooking hearth was deposited at the site between A.D. 1270 and A.D. 1400 but prior to the arrival of Spanish missionaries ca. 1775. A penultimate event probably occurred between A.D. 620 and A.D. 1400. These events were associated with displacements on the order of 3 m (and perhaps as much as 5 m). Our findings show that the fault trace takes a more arcuate path across the Seal Cove gap than is shown on previous mapping. The fault is associated with a 1.5- to 6-m-high east-facing scarp across the Seal Cove gap.

The results of this study show that the San Gregorio fault plays an active role in accomodating strain along the Pacific/North American plate margin and supports the model of a coastal system of strike-slip faults. The San Gregorio fault should be considered an active seismogenic source in local seismic hazard assessments. The fault has been accumulating strain for between 220 and 730 yr. If fault slip rate on the San Gregorio fault is on the order of 4 to 10 mm/yr, then 0.9 to 7.3 m of elastic strain has accrued since the last event.

Acknowledgments

We are indebted to Mark G. Hylkema and a large group of volunteers who conducted the archaeological investigation. We are thankful to Gerry Weber, Jeff Nolan, and Kent Lightfoot for their insights during the course of the study. Rick Zeeb and Carolyn Mosher did an outstanding job drafting the figures. Park ranger Bob Breen and the San Mateo County Department of Parks and Recreation were most gracious in allowing us to conduct this study within the Fitzgerald Marine Reserve. We thank Ken Lajoie and Jennifer Harden for thourough reviews that improved this article. Research was supported by the U.S. Geological Survey's National Earthquake Hazard Reduction program under Award #1434-94-G-2275. The views and conclusions contained in this report are those of the authors and should not be interpreted as necessarily representing the official policies, either expressed or implied, of the U.S. Government.

References

Bedrossian, T. L. (1979). Fault-evaluation report FER-93, *California Division of Mines and Geology unpublished report,* 9 pp. with plates.

Berger, R., R. E. Taylor, and W. F. Libby (1966). Radiocarbon content of marine shells from the California and Mexican west coast, *Science* **153,** 864–866.

Brabb, E. E. and E. H. Pampeyan (1972). Preliminary geologic map of San Mateo County, California, U.S. Geol. Surv. Basic Data Contribution 41, Map MF-328, scale 1:62,500.

Brocher, T. M. (1993). Seismogenic and potentially seismogenic structures imaged by wide-angle onshore-offshore seismic profiling of the western margin of North America (abstract), *EOS* **74,** no. 43, 431.

Clahan, K. B., R. H. Wright, and N. T. Hall (1995). Paleoseismic investigation of the San Andreas fault on the San Francisco Peninsula, CA, in *National Earthquake Hazards Reduction Program Annual Project Summaries: XXXVI,* M. L. Jacobsen (Editor), *U.S. Geol. Surv. Open-File Rept. 95-210.*

Clark, J. C., E. E. Brabb, H. G. Greene, and D. C. Ross (1984). Geology of Point Reyes Peninsula and implications for San Gregorio fault history, in *Tectonics and Sedimentation along the California Margin,* J. K. Crouch and S. B. Bachman (Editors), Pacific Section S.E.P.M., Vol. 38, 67–86.

Cleary Consultants (1990). Fault location investigation, interpretive center site, Fitzgerald Marine Reserve, San Mateo County, California, unpublished consultants report.

Coppersmith, K. J. and G. B. Griggs (1978). Morphology, recent activity, and seismicity of the San Gregorio fault zone, in *San Gregorio-Hosgri Fault Zone, California,* E. A. Silver and W. R. Normark (Editors), *California Division of Mines and Geology Special Report 137,* 33–44.

Galehouse, J. S. (1995). Theodolite measurements of creep rates on San Francisco Bay region faults, in *National Earthquake Hazards Reduction Program Annual Project Summaries: XXXVI,* M. L. Jacobsen (Editor), *U.S. Geol. Surv. Open-File Rept. 95-210,* 335.

Glen, W. (1959). Pliocene and lower Pleistocene of the western part of the San Francisco peninsula: University of California Publications in Geological Sciences, Vol. 36, no. 2, pp. 147–198, map scale approx. 1:44,000.

Graham, S. A. and W. R. Dickinson (1978). Apparent offsets of on-land geologic features across the San Gregorio-Hosgri fault trend, in *San Gregorio-Hosgri Fault Zone, California,* E. A. Silver and W. R. Normark (Editors), *California Division of Mines and Geology Special Report 137,* 13–23.

Greene, H. G., D. Orange, D. Mann, and G. Gable (1994). Fluid constructed morphology on Smooth Ridge, central California (abstract), *EOS,* 1994 Fall Meeting Abstract Supplement.

Hall, C. A., Jr. (1975). San Simeon-Hosgri fault system, coastal California: economic and environmental implications, *Science* **190,** 1291–1294.

Hill, D. P., *et al.* (1991). The seismotectonic fabric of central California, in *Neotectonics of North America,* D. B. Slemmons *et al.* (Editors), Geological Society of America Decade Map Volume 1, 107–132.

Hylkema, M. G. (1996). Seal Cove pre-history: archaeological investigations at CA-SMA-134, Fitzgerald Marine Reserve, San Mateo County, CA: On file at the Historical Resources Information System, Northwest Information Center, Sonoma State University, Rohnert Park, California.

Jack, R. N. (1969). Quaternary sediments of the Montara Mountain area, San Mateo County, California, unpublished *Master's Thesis,* University of California, Berkeley, map.

JCP Associates (1987). Engineering geologic, soil and foundation study for four proposed residences on Orval Avenue, Moss Beach, San Mateo County, CA, unpublished consultants report.

Jennings, C. W. (1994). Fault activity map of California and adjacent areas: California Geological Data Map Series, California Division of Mines and Geology, map no. 6.

Kelson, K. I., W. R. Lettis, and M. Lisowski (1992). Distribution of geologic slip and creep along faults in the San Francisco Bay region: in *Proc. of the 2nd Conference on Earthquake Hazards in the Eastern San Francisco Bay Area,* G. Borchardt *et al.* (Editors), *California Division of Mines and Geology, Special Publication 113,* 31–38.

Kennedy, G. L., K. R. Lajoie, D. J. Blunt, and S. A. Mathieson (1981). Half Moon Bay terrace, California, and the age of its Pleistocene invertebrate faunas, *Western Society of Malacologists Annual Report,* **14,** 2 pp.

Lajoie, K. R. (1986). Coastal Tectonics, in *Active Tectonics,* National Academy Press, Washington, D.C., 95–124.

Lajoie, K. R., G. E. Weber, S. Mathieson, and J. Wallace (1979). Quaternary tectonics of coastal Santa Cruz and San Mateo Counties, California, as indicated by deformed marine terraces and alluvial deposits, in *Field Trip Guidebook to Coastal Tectonics and Coastal Geologic Hazards in Santa Cruz and San Mateo Counties, California,* G. E. Weber, K. R. Lajoie, and G. B. Griggs (Editors), *Geological Society of America Cordilleran section,* 61–80.

Leighton, F. Beach and Associates (1971). Final engineering geologic report of the Seal Cove-Moss Beach area, County of San Mateo, unpublished consulting report prepared for the County of San Mateo, 16 pp. plus figures and appendices.

Lewis, S. D. (1993). Central California continental margin crustal structure from depth-migrated reflection profiles (abstract), *EOS,* 1994 Fall Meeting Abstract Supplement.

Lewis, S. D. (1994). Seismic reflection profiles of folds and thrust faults, offshore San Francisco region (abstract), *EOS,* 1994 Fall Meeting Abstract Supplement.

Niemi, T. M. and N. T. Hall (1992). Late Holocene slip rate and recurrence of great earthquakes on the San Andreas fault in northern California, *Geology* **20,** 195–198.

Noller, J. S., K. I. Kelson, W. R. Lettis, K. A. Wickens, G. D. Simpson, K. Lightfoot, and T. Wake (1993). Preliminary characterization of Holocene activity on the San Andreas fault based on offset archaeologic sites, Ft. Ross State Historic Park, California, Final Technical Report for *U.S. Geol. Surv. National Earthquake Hazard Reduction Program,* 16 pp.

Pampeyan, E. H. (1994). Geologic Map of the Montara Mountain and San Mateo Quadrangles, San Mateo County, California, U.S. Geol. Surv. Misc. Invest. Series Map I-2390, scale 1:24,000.

Reed, D. L., C. McHugh, and W. B. F. Ryan (1992). MSSS-1 survey of the offshore San Gregorio fault system: implications for recent displacement (abstract), *EOS* **73,** no. 43, 589.

Robinson, S. W. and G. Thompson (1981). Radiocarbon corrections for marine shell dates with application to southern Pacific northwest coast prehistory, *Syesis* **14,** 45–57.

Sedlock, R. L. and D. H. Hamilton (1991). Late Cenozoic tectonic evolution of southwestern California, *J. Geophys. Res.* **96,** no. B2, 2325–2351.

Stuiver, M. and P. J. Reimer (1993). Radiocarbon calibration program "Calib 3.0.3," *Radiocarbon* **35,** 215–230.

Stuiver, M., G. W. Pearson, and T. F. Braziunas (1986). Radiocarbon age calibration of marine samples back to 9000 cal yr B.P., *Radiocarbon* **28,** 980–1021.

Toppozada, T. R., C. R. Real, and D. L. Parke (1981). Preparation of isoseismal maps and summaries of reported effects for pre-1900 California earthquakes, *Calif. Div. Mines Geol. Open-File Rept. 81-11,* 182 pp.

Weber, G. E. (1994). Late Pleistocene slip rates on the San Gregorio fault zone at Point Año Nuevo, San Mateo County, California, in *Field Trip Guidebook to Transpressional Deformation in the San Francisco Bay Region,* William R. Lettis (Editor), Friends of the Pleistocene, Pacific Southwest Cell.

Weber, G. E. and W. R. Cotton (1981). Geologic investigation of recurrence intervals and recency of faulting along the San Gregorio fault zone, San Mateo County, California, *U.S. Geol. Surv. Open-File Rept. 81-263,* 129 pp.

Weber, G. E. and K. R. Lajoie (1980). Map of Quaternary faulting along the San Gregorio fault zone, San Mateo and Santa Cruz counties, California, *U.S. Geol. Surv. Open-File Rept. 80-907,* sheet 1 of 3, scale 1:24,000.

Wells, D. L. and K. J. Coppersmith (1994). New empirical relationships among magnitude, rupture length, rupture width, rupture area, and surface displacement, *Bull. Seism. Soc. Am.* **84,** 974–1002.

WGCEP (Working Group on California Earthquake Probabilities) (1990). Probabilities of large earthquakes in the San Francisco Bay region, California, *U.S. Geol. Surv. Circular 1053,* 51 pp.

Wood, P. R. (1983). Geologic reconnaissance, lots 19 and 20, Marine Avenue and Beach Way, Moss Beach, San Mateo County, California, unpublished consultants report.

William Lettis & Associates, Inc.,
1777 Botelho Dr., #262
Walnut Creek, California 94596

Manuscript received 1 July 1996.